



Published in final edited form as:

*Biochem Biophys Res Commun.* 2019 January 01; 508(1): 87–91. doi:10.1016/j.bbrc.2018.11.083.

## Interleukin-6 derived from cutaneous deficiency of stearoyl-CoA desaturase- 1 may mediate metabolic organ crosstalk among skin, adipose tissue and liver

Sabrina N Dumas<sup>#1</sup>, Chang-an Guo<sup>#2</sup>, Jason K. Kim<sup>3,4</sup>, Randall H. Friedline<sup>3,4</sup>, and James M Ntambi<sup>1,2,\*</sup>

<sup>1</sup>Department of Nutritional Sciences, University of Wisconsin-Madison, Madison, Wisconsin 53706

<sup>2</sup>Department of Biochemistry, University of Wisconsin-Madison, Madison, Wisconsin 53706

<sup>3</sup>Program in Molecular Medicine, University of Massachusetts Medical School, Worcester, Massachusetts, USA

<sup>4</sup>Division of Endocrinology, Metabolism, and Diabetes, Department of Medicine, University of Massachusetts Medical School

# These authors contributed equally to this work.

### Abstract

Stearoyl-CoA desaturase 1 (SCD1), a lipogenic enzyme that adds a double bond at the delta 9 position of stearate (C18: 0) and palmitate (C16: 0), has been proven to be important in the development of obesity. Mice with skin-specific deficiency of SCD1 (SKO) display increased whole-body energy expenditure, which is protective against adiposity from a high-fat diet because it improves glucose clearance, insulin sensitivity, and hepatic steatosis. Of note, these mice also display elevated levels of the “pro- inflammatory” plasma interleukin-6 (IL-6). In whole skin of SKO mice, IL-6 mRNA levels are increased, and protein expression is evident in hair follicle cells and in keratinocytes. Recently, the well-known role of IL-6 in causing white adipose tissue lipolysis has been linked to indirectly activating the gluconeogenic enzyme pyruvate carboxylase 1 in the liver, thereby increasing hepatic glucose production. In this study, we suggest that skin-derived IL-6 leads to white adipose tissue lipolysis, which contributes to the lean phenotype of SKO mice without the incidence of meta- inflammation that is associated with IL-6 signaling.

### Introduction

Stearoyl-CoA desaturase-1 (SCD) is an endoplasmic reticulum enzyme that controls the addition of a double bond at the delta-9 position of saturated fatty acids (SFA) to make monounsaturated fatty acids (MUFA) (1). SCD1 favors palmitate (16:0) and stearate (18:0)

\*Corresponding author: james.ntambi@wisc.edu.

**Publisher's Disclaimer:** This is a PDF file of an unedited manuscript that has been accepted for publication. As a service to our customers we are providing this early version of the manuscript. The manuscript will undergo copyediting, typesetting, and review of the resulting proof before it is published in its final citable form. Please note that during the production process errors may be discovered which could affect the content, and all legal disclaimers that apply to the journal pertain.

as substrates to produce palmitoleate (16:1n7) and oleate (18:1n9), respectively (1). SCD1-derived MUFAs are integral to health because palmitoleate and oleate are incorporated into such key lipids as phospholipids, triglycerides, cholesterol esters, and wax esters (1). Interestingly, deletion of SCD1 in mice leads to decreased risk for developing metabolic diseases: SCD1<sup>-/-</sup> mice are lean, insulin sensitive, glucose tolerant, and resistant to developing fatty liver (2).

However, conversion of SFAs into MUFAs also has a protective anti-inflammatory role because it decreases the pool of SFA available for binding toll-like receptor 4 (TLR4) (3). Signaling through TLR4 leads to production of cytokines such as interleukin-1 (IL-1), interleukin-6 (IL-6), and tumor necrosis factor alpha (TNF $\alpha$ ) (4). Cytokine production is especially of interest with SCD1-deficient mice because many reports suggest that SCD1 inhibition promotes inflammation (5), which is in agreement with accumulating levels of SFAs when SCD1 is inhibited. Because SCD1 is a potential therapeutic target for combating metabolic disease (6), SCD1-mediated cytokine production must be better understood before any clinical development can take place.

In this study, we focus on skin-specific SCD1 deficiency because these mice recapitulate the metabolic advantages of global SCD1 deficiency while keeping SCD1 expression intact in all other tissues (7). As a result, SKO mice have fewer negative side effects compared to global SCD1-deficient mice (GKO), such as hypercholesterolemia, cholestasis, and hypoglycemia (8).

Several mechanisms have been proposed to explain the hypermetabolic phenotypes of SKO mice, such as heat/water loss or adipose browning due to significantly reduced fur and sebaceous lipid coverage on SKO skins (9). However, when SKO mice were housed under thermoneutral conditions at 33°C, SKO mice were still hyperphagic in comparison to WT counterparts and were still resistant to weight gain (10). This surprising SKO mouse phenotype emphasizes that additional mechanisms within skin exist and are critical to the regulation of whole-body energy homeostasis.

In order to identify a potential skin-derived factor produced by SKO mice, we revisited our previously published dataset of genes altered in SKO skin (10). In this report, transcripts of several cytokines including *Il1*, *Il18*, *Il5*, *Il-6*, and *Il8* were significantly elevated (10). We hypothesized that IL-6 may be a mediator regulating organ crosstalk in SKO mice for two main reasons: 1) overexpression of IL-6 in skin leads to the development of alopecia with age, a phenotype shared with SKO mice (11) and 2) IL-6 overexpression has been shown to decrease whole-body adiposity, which is yet another similarity with SKO mice (12).

IL-6 is best known for its role in maturing naïve B cells into antibody-producing cells, a fundamental process in acquired immunity (13). However, IL-6 function varies depending on cell type and is widely regarded as a multifunctional cytokine (14). Furthermore, IL-6 is expressed by a variety of cell types outside of the immune system, including (but not limited to) adipocytes, hepatocytes, and keratinocytes (15). In white adipocytes, IL-6 expression leads to lipolysis through activation of the JAK-Stat signaling pathway and a resulting inability to accumulate lipids in fat pads (16). In hepatocytes, activity of gluconeogenic

enzymes and inflammation are suppressed; in keratinocytes, IL-6 promotes proliferation (15, 17).

The effects of IL-6 signaling also vary depending on which IL-6 receptor is activated. The IL-6 receptor has no independent signaling properties and instead relies on heterodimerization with another membrane protein, gp130, which is expressed almost ubiquitously (18). Gp130 has no affinity for free IL-6 and only binds to the IL-6:IL-6R receptor complex (18). IL-6 receptors are either membrane-bound or soluble; membrane-bound IL-6 receptor expression is limited to liver, leukocytes, and some epithelial barrier cells (18). However, tissues without membrane bound IL-6 receptor are still responsive to the IL-6:IL-6R complex because gp130 can bind to either the membrane-bound or free version of the IL-6R (18). As a result, IL-6 signaling can occur in a variety of tissues. In this study, we suggest that IL-6 mediates white adipose tissue lipolysis, which leads to decreased adiposity—thereby suggesting that IL-6 has a positive role in the context of skin-specific SCD1 deficiency.

## Materials and Methods

### Animals and Diets

Generation and maintenance of *Scd1f/f* and SKO mouse lines have been described previously (7). Mice were maintained on a 12-hour light/dark cycle with free access to water and a high-fat diet (Research Diets D12492) for 8, 9, or 10 weeks. Breeder mice were maintained with similar conditions but fed breeder chow diet (Purina 5015). All animals were sacrificed by isoflurane overdose without fasting; tissues and plasma were quickly removed, snap-frozen in liquid nitrogen, and stored at  $-80^{\circ}\text{C}$ . Skin tissue was harvested whole and included both the dermis and epidermis. All animal procedures were approved by the Animal Care Research Committee of the University of Wisconsin-Madison.

### Quantitative real-time PCR

Total skin RNA was extracted using TRI reagent, which was then treated with Turbo DNase (Ambion) and followed by reverse transcription into cDNA using a High-Capacity cDNA Reverse Transcription Kit (Applied Biosystems). Relative mRNA expression levels were quantified by cDNA amplification with gene-specific forward and reverse primers and Power SYBR Green PCR Master Mix on an ABI 7500 Fast RT PCR system. Data were normalized to cyclophilin using the  $\Delta\Delta\text{Ct}$  method. Primer sequences are available upon request.

### Immunohistochemistry

Fresh skin tissue was frozen in OCT compound and cut into 10-micron sections and stained with either IL-6 (ab6672) or F4-80 (ab6640) at a 1:250 dilution. Images were obtained using a Nikon Intensilight Fluorescence Microscope. Sectioning and staining of tissue was performed at the UWCCC Experimental Pathology Laboratory.

### Detection of cytokines

Blood was collected from mice via cardiac puncture. Serum was prepared within 30 minutes and frozen at  $-80^{\circ}\text{C}$  until use. The cytokine content of each sample was measured by multiplex assay, according to manufacturer's instructions (MILLIPLEX MAP Mouse Cytokine/Chemokine Magnetic Bead Panel, Merck Millipore, Massachusetts, USA). Standard curves were generated using the specific standards supplied by the manufacturer. Samples were analyzed on a MAGPIX<sup>®</sup> system (Millipore) using the MILLIPLEX<sup>®</sup> Analyst 5.1 software. The customized cytokine panel included IL-1alpha, IL-1beta, IL-4, IL-6, IL-10, IFN-gamma, GM-CSF, KC(IL-8), TNF- alpha, FGF-21, Leptin, Adiponectin.

### Ex vivo lipolysis assay in adipose tissue explants.

Epididymal fat pads were surgically removed from male mice and washed with ice-cold PBS. Fat pads (100 mg, n = 4/mouse) were preincubated for 1 h in 140  $\mu\text{l}$  of DMEM (Life Technologies) containing 2% fatty acid-free serum albumin (Sigma-Aldrich). Subsequently, fat pads were incubated in 250  $\mu\text{l}$  of KRH buffer (125 mM NaCl, 5 mM KCl, 1.8 mM  $\text{CaCl}_2$ , 2.6 mM  $\text{MgSO}_4$ , 5 mM HEPES, pH 7.2) plus 2% BSA (fatty acid free) for 2h at  $37^{\circ}\text{C}$ . Free glycerol content was quantified for each sample in the medium using the Free Glycerol Determination Kit (Wako Diagnostics). Glycerol release from each sample was normalized to the weight of each fat pad.

### Pyruvate Tolerance Test

After 9 hours of fasting, 8-week-old mice on a HFD for 7 or 8 weeks were injected intraperitoneally with sterile sodium pyruvate (2g/kg). Levels of blood glucose were measured at 15, 30, 60, 90, and 120 minutes using blood collected from the tail vein. An automatic glucose monitor was used to record blood glucose readings (OneTouch; LifeScan).

### Pyruvate Carboxylase Activity Assay

Pyruvate carboxylase activity was measured by a coupled spectrophotometric assay as described previously (19). Oxaloacetate formed by the action of pyruvate carboxylase in the presence of excess citrate synthase (Sigma) reacts with acetyl-CoA to yield citrate and to liberate free CoA. This free CoA stoichiometrically reduces added 5,5- dithiobis(z-nitrobenzoic acid) (DTNB, Sigma) to yield a colored product.

### Statistics

Data are expressed as mean  $\pm$  S.E. with comparisons carried out using a two-sided Student's t-test using the program GraphPad Prism. p values  $<0.05$  were considered significant.

## Results

### Proinflammatory M1 macrophages and IL-6 are increased in SKO skin.

We have previously reported that SCD1 is involved in the regulation of inflammation and stress in macrophages, white adipocytes, and endothelial cells (5). In the current study, we

further analyzed the expression of macrophage markers *cd68*, *cd11b*, *cd11c*, *mg11*, and *il-6* in skin. *Cd11c* is a marker of proinflammatory M1 macrophages whereas *mg11* is a marker of anti-inflammatory M2 macrophages. We found that M1 (*CD11c*) but not M2 (*MGL1*) macrophages were elevated in SKO skin (Figure 1a). M1 macrophages are known to secrete IL-6; in agreement, levels of IL-6 mRNA are also significantly increased (Figure 1a), which also validated our previously published microarray data (10). *Cd68* and *cd11b* are markers for total macrophages: both are unchanged. To assess protein expression of macrophages, we stained frozen skin sections for F4–80, a routinely used marker of macrophage infiltration (19). We found increased staining localized around the hair follicles of SKO mice (Figure 1b). We followed up with IL-6 staining and found that IL-6 expression was also localized around hair follicles (Figure 1c). Interestingly, IL-6 expression also colocalized with keratinocyte hyperproliferation along the epidermis (Figure 1c).

### Levels of both plasma IL-6 and white adipose tissue lipolysis are increased in SKO mice.

IL-6 as a cytokine is present in plasma under conditions of acute and chronic inflammation (20). Because IL-6 is clearly elevated within the whole skin of SKO mice, we measured levels of IL-6 in the blood using Luminex bead-based multiplex assay, which involved measurements of a panel of cytokines, including IL-1 $\alpha$ , IL-1 $\beta$ , IL-4, IL-6, IL-10, IFN $\gamma$ , IL-8, TNF, FGF21, leptin, and adiponectin. As expected, levels of IL-6 were dramatically increased—25-fold—in SKO mice (Figure 2a). Because IL-6 is a well-known lipolytic agent of adipose tissue (16), we measured levels of glycerol release in the explants of epididymal white adipose tissue (eWAT). SKO mice displayed significantly higher levels of eWAT lipolysis as indicated by increased levels of free glycerol in the *ex vivo* lipolysis assay of eWAT fat pads (Figure 2b).

### Hepatic gluconeogenesis is elevated in SKO mice.

White adipose tissue-derived free fatty acids (FFA) have recently been shown to play a role in the activation of hepatic gluconeogenesis (21). We hypothesized that in SKO mice, the increased release of FFA from adipose tissue by circulating IL-6 will activate the hepatic glucose production program. To investigate, we injected SKO mice with pyruvate, which is a well-established gluconeogenic substrate (22). At the time of injection, SKO mice were on a HFD for 7 or 8 weeks: in both groups, concentrations of blood glucose increased dramatically at the 30-minute mark (Figure 3a and b). The additional week of HFD feeding correlated with increased levels of glucose production in both *SCD1f/f* and SKO mice. The combination of data for both cohorts of mice demonstrate a sharp increase in hepatic glucose production at the 30-minute mark (Figure 3c). Interestingly, SKO mice were also able to rapidly clear blood glucose after 30 minutes, which agrees well with work previously published from our lab outlining enhanced glucose tolerance of SKO mice (7). Hepatic  $\beta$ -oxidation of free fatty acids sourced from eWAT generates acetyl CoA, which is known to activate a key gluconeogenic enzyme, pyruvate carboxylase 1 (PC1) (21). For this reason, we measured the activity of PC1 in livers from SKO mice: we found a significant increase in PC1 activity (Figure 4a and b).

## Discussion

Our previous work presented hallmarks of GKO and SKO mouse models, including both hypermetabolic phenotype and hypersensitivity to insulin signaling (2,7). Though these phenotypes might be beneficial to obesity, they pose a constant risk of hypoglycemia to lean individuals. The current study emphasizes a pivotal role of skin in regulating a crosstalk among distant metabolic organs by IL-6 and illustrates a novel strategic mechanism in these animals that promotes the hepatic gluconeogenesis program and maintains a status of euglycemia. We propose that skin-specific SCD1 deficiency leads to increased expression of IL-6 locally in the skin, which then contributes to decreased whole-body adiposity. We formulated this hypothesis based on the observation that IL-6 mRNA in skin is significantly elevated in a mouse model that, similar to IL-6 over-expressing mice, does not have the ability to expand white adipose tissue depots (11,12). We then supported the hypothesis that IL-6-mediated eWAT lipolysis occurs in SKO mice by confirming increased hepatic PC1 activity and, as a result, increased gluconeogenesis.

IL-6 has been linked to a variety of health and disease states; there is no shortage of information supporting both positive (anti-inflammatory) and negative (proinflammatory) roles for IL-6 (15). However, there is evidence that *cis*-signaling through the membrane-bound IL-6R is anti-inflammatory, whereas *trans*-signaling through the soluble IL-6R is proinflammatory (18). For example, *cis*-signaling in hepatocytes leads to decreased inflammation, but increased *trans*-signaling is ineffective (23). In muscle, IL-6 is known to enhance muscle efficiency and growth through a process that involves stimulating glycogenolysis and lipolysis (24). Muscle-derived IL-6 can also signal through the L cells of the small intestines to induce glucagon-like peptide 1 (GLP-1) secretion into plasma. GLP-1 can then travel to the pancreases and mediate  $\beta$ -cell expansion, which then leads to increased insulin secretion (25). More research needs to be done before IL-6 can be targeted to improve metabolic health. But a possible next step for SKO research would be to assess the levels of *trans*- and *cis*-signaling taking place in the skin, eWAT, and livers of SKO mice to determine whether IL-6 truly has an anti-inflammatory role.

## Acknowledgements

Histology and immunohistochemistry were conducted at the UW Carbone Cancer Center Experimental Pathology Laboratory, Madison, WI. This work was supported by National Institutes of Health (NIH) Grant R01 DK062388, ADA 7-13-BS-118, and USDA Hatch W2005 (to J.M.N.), United States Department of Agriculture (USDA) Hatch W2005 (to J.M.N.) and University of Wisconsin-Madison's Science and Medicine Graduate Research Scholars (SciMed GRS) (to S.N.D). The cytokine content of each sample was measured by multiplex assay conducted at the National Mouse Metabolic Phenotyping Center at UMass Medical School, funded by an NIH grant 5U2C-DK093000 (to J.K.K.)

## References

1. Paton CM and Ntambi JM, 2009 Biochemical and physiological function of stearoyl-CoA desaturase. *American Journal of Physiology-Endocrinology and Metabolism*, 297(1), pp.E28–E37. [PubMed: 19066317]
2. Ntambi JM, Miyazaki M, Stoehr JP, Lan H, Kendziorski CM, Yandell BS, Song Y, Cohen P, Friedman JM and Attie AD, 2002 Loss of stearoyl-CoA desaturase-1 function protects mice against adiposity. *Proceedings of the National Academy of Sciences*, 99(17), pp.11482–11486.

3. Lee JY, Sohn KH, Rhee SH and Hwang D, 2001 Saturated fatty acids, but not unsaturated fatty acids, induce the expression of cyclooxygenase-2 mediated through Toll-like receptor 4. *Journal of Biological Chemistry*, 276(20), pp.16683–16689. [PubMed: 11278967]
4. Lu YC, Yeh WC and Ohashi PS, 2008 LPS/TLR4 signal transduction pathway. *Cytokine*, 42(2), pp. 145–151. [PubMed: 18304834]
5. Liu X, Strable MS and Ntambi JM, 2011 Stearoyl CoA desaturase 1: role in cellular inflammation and stress. *Advances in nutrition*, 2(1), pp.15–22. [PubMed: 22211186]
6. Dobrzyn A and Ntambi JM, 2005 Stearoyl-CoA desaturase as a new drug target for obesity treatment. *Obesity Reviews*, 6(2), pp.169–174. [PubMed: 15836467]
7. Sampath H, Flowers MT, Liu X, Paton CM, Sullivan R, Chu K, Zhao M and Ntambi JM, 2009 Skin-specific deletion of stearoyl-CoA desaturase-1 alters skin lipid composition and protects mice from high fat diet-induced obesity. *Journal of Biological Chemistry*, 284(30), pp.19961–19973. [PubMed: 19429677]
8. Flowers MT, Groen AK, Oler AT, Keller MP, Choi Y, Schueler KL, Richards OC, Lan H, Miyazaki M, Kuipers F and Kendzioriski CM, 2006 Cholestasis and hypercholesterolemia in SCD1-deficient mice fed a low-fat, high- carbohydrate diet. *Journal of lipid research*, 47(12), pp.2668–2680. [PubMed: 17005996]
9. Nedergaard J and Cannon B, 2014 The browning of white adipose tissue: some burning issues. *Cell metabolism*, 20(3), pp.396–407. [PubMed: 25127354]
10. Flowers MT, Paton CM, O'Byrne SM, Schiesser K, Dawson JA, Blaner WS, Kendzioriski C and Ntambi JM, 2011 Metabolic changes in skin caused by Scd1 deficiency: a focus on retinol metabolism. *PloS one*, 6(5), p.e19734. [PubMed: 21573029]
11. Turksen K, Kupper T, Degenstein L, Williams I and Fuchs E, 1992 Interleukin 6: insights to its function in skin by overexpression in transgenic mice. *Proceedings of the National Academy of Sciences*, 89(11), pp.5068–5072.
12. Peters M, Schirmacher P, Goldschmitt J, Odenthal M, Peschel C, Fattori E, Ciliberto G, Dienes HP, Zum Büschenfelde KHM and Rose-John S, 1997 Extramedullary expansion of hematopoietic progenitor cells in interleukin (IL)-6-sIL-6R double transgenic mice. *Journal of Experimental Medicine*, 185(4), pp.755–766. [PubMed: 9034153]
13. Kishimoto T and Tanaka T, 2015 Interleukin 6. *Encyclopedia of Inflammatory Diseases*, pp.1–8.
14. Liu X, Jones GW, Choy EH and Jones SA, 2016 The biology behind interleukin-6 targeted interventions. *Current opinion in rheumatology*, 28(2), pp.152–160. [PubMed: 26751841]
15. Mauer J, Denson JL and Brüning JC, 2015 Versatile functions for IL-6 in metabolism and cancer. *Trends in immunology*, 36(2), pp.92–101. [PubMed: 25616716]
16. Hu W, Lv J, Han M, Yang Z, Li T, Jiang S and Yang Y, 2018 STAT3: The art of multi-tasking of metabolic and immune functions in obesity. *Progress in lipid research*.
17. Ramadoss P, Unger-Smith NE, Lam FS and Hollenberg AN, 2009 STAT3 targets the regulatory regions of gluconeogenic genes in vivo. *Molecular endocrinology*, 23(6), pp.827–837. [PubMed: 19264844]
18. Lacroix M, Rousseau F, Guilhot F, Malinge P, Magistrelli G, Herren S, Jones SA, Jones GW, Scheller J, Lissilaa R and Kosco-Vilbois M, 2015 Novel insights into interleukin 6 (IL-6) cis- and trans-signaling pathways by differentially manipulating the assembly of the IL-6 signaling complex. *Journal of Biological Chemistry*, 290(45), pp.26943–26953. [PubMed: 26363066]
19. Spiller KL, Anfang RR, Spiller KJ, Ng J, Nakazawa KR, Daulton JW and Vunjak-Novakovic G, 2014 The role of macrophage phenotype in vascularization of tissue engineering scaffolds. *Biomaterials*, 35(15), pp.4477–4488. [PubMed: 24589361]
20. Pradhan AD, Manson JE, Rifai N, Buring JE and Ridker PM, 2001 C- reactive protein, interleukin 6, and risk of developing type 2 diabetes mellitus. *Jama*, 286(3), pp.327–334. [PubMed: 11466099]
21. Perry RJ, Camporez JPG, Kursawe R, Titchenell PM, Zhang D, Perry CJ, Jurczak MJ, Abudukadier A, Han MS, Zhang XM and Ruan HB, 2015 Hepatic acetyl CoA links adipose tissue inflammation to hepatic insulin resistance and type 2 diabetes. *Cell*, 160(4), pp.745–758. [PubMed: 25662011]

22. Rognstad R, 1976 Control of pyruvate kinase flux during gluconeogenesis in isolated liver cells. *International Journal of Biochemistry*, 7(8), pp.403–408.
23. Baran P, Hansen S, Waetzig GH, Akbarzadeh M, Lamertz L, Huber HJ, Ahmadian MR, Moll JM and Scheller J, 2018 The balance of Interleukin (IL)-6, IL-6: soluble IL-6 receptor (IL-6R) and IL-6: sIL-6R: sgp130 complexes allows simultaneous classic and trans-signaling. *Journal of Biological Chemistry*, pp.jbc-RA117.
24. Keller C, Keller P, Marshal S and Pedersen BK, 2003 IL-6 gene expression in human adipose tissue in response to exercise–Effect of carbohydrate ingestion. *The Journal of physiology*, 550(3), pp.927–931. [PubMed: 12794182]
25. Ellingsgaard H, Hauselmann I, Schuler B, Habib AM, Baggio LL, Meier DT, Eppler E, Bouzakri K, Wueest S, Muller YD and Hansen AMK, 2011 Interleukin-6 enhances insulin secretion by increasing glucagon-like peptide-1 secretion from L cells and alpha cells. *Nature medicine*, 17(11), p.1481.



### Highlights

1. IL-6 expression is significantly increased in the skin of skin-specific SCD1 deficient (SKO) mice and is also dramatically elevated in blood.
2. White adipose tissue lipolysis, a well-known effect of IL-6, is evident in SKO mice.
3. White-adipose tissue derived hepatic acetyl-CoA is known to increase hepatic gluconeogenesis by activating pyruvate kinase; both PC1 activity and gluconeogenesis are increased in SKO mice.

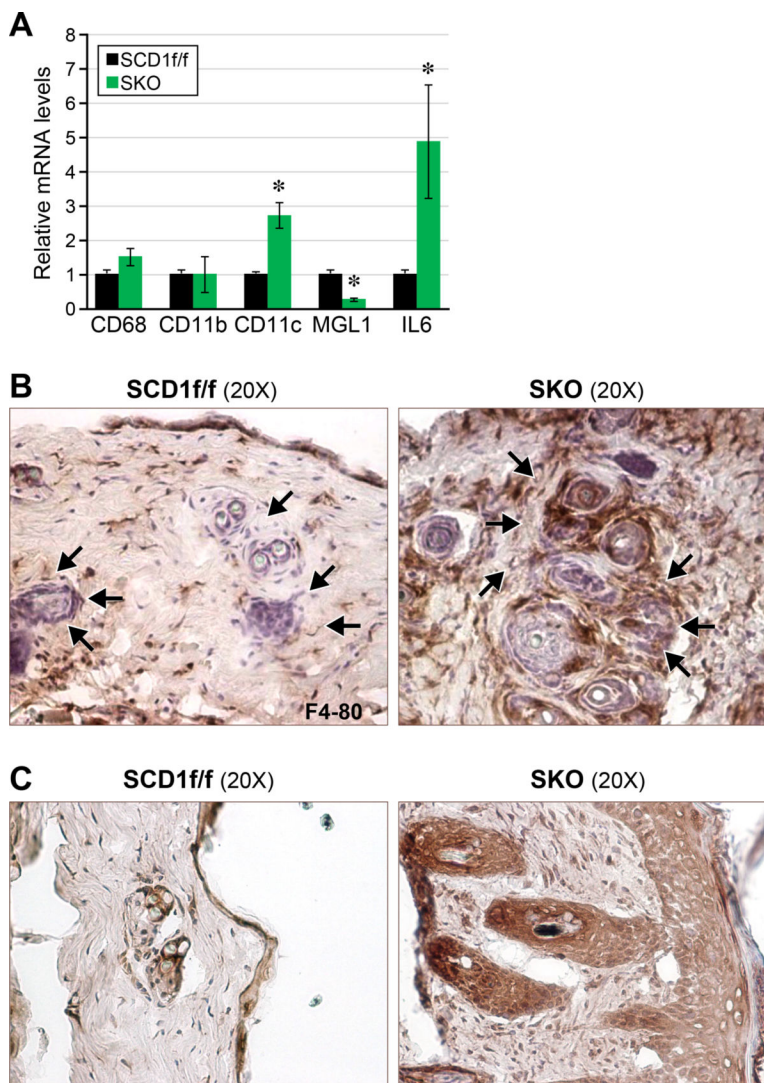


**Figure 1.** Proinflammatory M1 macrophages and IL-6 are increased in SKO skin. (a) Levels of M1 macrophages and IL-6 are increased in whole skin of SKO mice. (b) Expression of F4-80 is localized around the hair follicles of SKO mice. (c) Expression of IL-6 is localized around both hair follicles and keratinocytes.

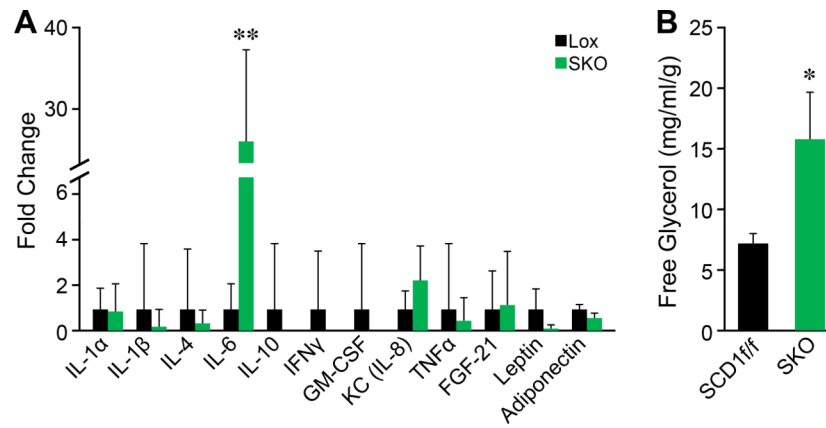


**Figure 2.** Levels of both plasma IL-6 and white adipose tissue lipolysis are increased in SKO mice. (a) IL-6 is increased by 25-fold in plasma of SKO mice. (b) Epididymal white adipose tissue lipolysis is increased as measured by levels of glycerol released from stored triglycerides.

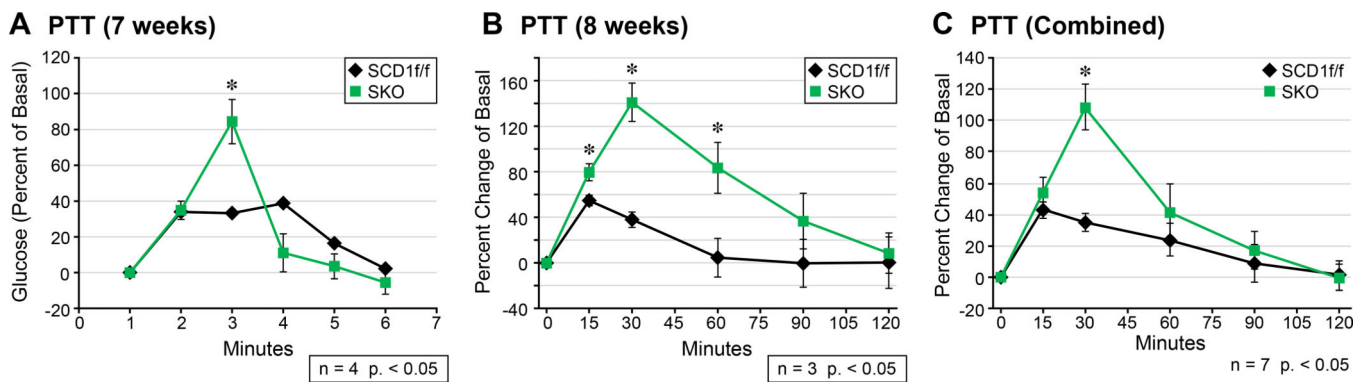


**Figure 3.** Pyruvate tolerance test (percent change of basal glucose levels). (a) Hepatic glucose production is sharply increased at 30 minutes and is rapidly cleared in SKO mice at 7 weeks; (b) the same trend is seen at 8 weeks; (c) combined data from (a) and (b).

Author Manuscript

Author Manuscript

Author Manuscript

Author Manuscript

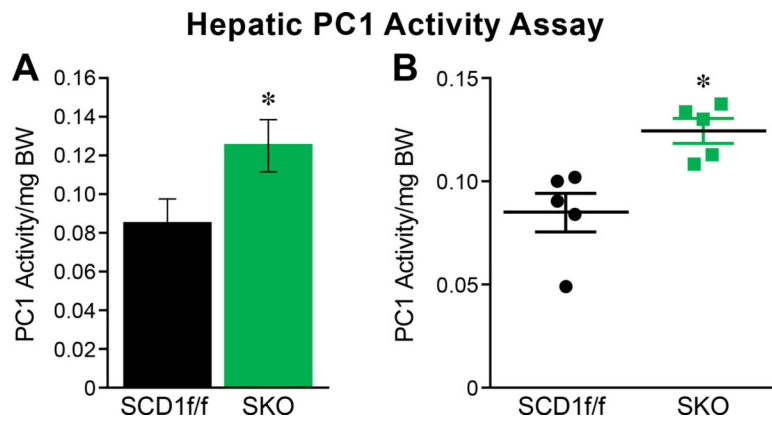


**Figure 4.** Hepatic PC1 activity is increased. The activity of gluconeogenic enzyme pyruvate carboxylase 1 (PC1) is increased in the livers of SKO mice fed a HFD.